Dufour Effect on MHD Free Convection Heat and Mass Transfer Effects Flow over an Inclined Plate Embedded in a Porous Medium

S. H. Islam[1*], P. Begum[2], D. Sarma[2]

[1]Department of Mathematics, Cotton Collegiate Govt. H. S. School, Guwahati, Assam, India

[2]Department of Mathematics, Cotton University, Guwahati, Assam, India

Abstract

The aim of this study is to present an exact analysis the effect of heat generation parameter and Dufour number on the magneto hydrodynamic (MHD) free convection flow of an electrically conducting incompressible viscous fluid over an inclined plate embedded in a porous medium. The impulsively started plate with variable temperature and mass diffusion is considered. The dimensionless momentum equation coupled with the energy and mass diffusion equations are analytically solved using the closed analytical method. Expressions for velocity, temperature and concentration fields are obtained. They satisfy all imposed initial and boundary conditions and can be reduced, as special cases, to some known solutions from the literature. Expressions for skin friction, Nusselt number and Sherwood number are also obtained. Finally, the effects of parameters on velocity, temperature and concentration profiles and skin friction coefficient are graphically displayed.

1. Introduction

The studies related to heat and mass transfer with magneto hydrodynamic (MHD) flow over an inclined plate has generated much interest from renewable energy systems, astrophysical and also hypersonic aerodynamics researchers for a number of decades. MHD are branches of continuum Mechanics, often drawing upon much the same mathematics and yielding many-closely related results. Moreover, it is fundamental to many fascinating areas in geophysics and astrophysics, and has a wide variety of human and laboratory or engineering applications. Several alternative terms have been used to denote MHD, such as magneto gas dynamics, magneto-fluid mechanics and hydrodynamics. MHD is often impressive for its complexity. Thus MHD is concerned with the study of the dynamics of electrically conducting fluids and plasmas (at ordinary temperature a gas is electrically non-conducting. But at a very high temperature (10000

---

* *Corresponding author:* hamidul705@gmail.com

degree Celsius) the gas becomes significantly ionized and electrically conducting. In such state the gas is known as plasma in a magnetic field. Several researchers investigated MHD flow through a fluid saturated porous and non-porous medium near vertical plate considering different aspects of the problem. Relevant studies are due to Raptis *et al.* [1], Yen and Chang [2], Chamkha [3], Mahapatra *et al.* [4], Munshi and Alim [5] etc .

Heat transfer is the science which predicts temperature distributions, which may be functions of both spatial coordinates and time, within regions of matter. Heat transfer also predicts the rate at which energy is transferred across a surface of interest due to temperature gradients at the surface and temperature difference between different surfaces. Thus heat transfer is thermal energy in transit due to a temperature difference. Whenever there exists a temperature difference in a medium or between media, heat transfer must occur. The amount of heat transfer per unit area, per unit time is the heat flux. Examples of the application of heat transfer principles are evident in the calculation of thermal stresses within a turbine blade in a jet engine, since these are determined by the temperature distribution, and in the determination of the size of a heat exchanger needed to produce a given heat transfer rate between the fluids separated by the exchanger walls. Another application of heat transfer include the design of combustors in internal combustion engines, heat treatment processes, the calculation of building energy loads needed to size the furnace or air conditioner, and the determination of cooling water requirements for electric power plants.

When a system contains more than one component whose species concentrations are different for various points, then there is a natural tendency for mass transfer, minimizing the concentration differences within the system. The transport of one constituent from a region of higher concentration to that of a lower concentration is called mass transfer. Mass transfer will take place as long as a difference in species concentration exists. Therefore, species concentration gradient in a mixture provides the driving potential for transport of that species. Examples of mass transfer are legion. For instance, a lump of sugar added to a cup of black coffee ventually dissolves and then diffuses uniformly throughout the coffee. Water evaporates from ponds to increase the humidity of the passing air stream, perfume presents a pleasant fragrance that is imparted throughout the surrounding atmosphere, dispersion of oxides of sulfur released from a power plant smoke stack into the environment are some of the examples of mass transfer. In several practical situations such as chemical reaction, evaporation and condensation the heat transfer process is always accompanied by the mass transfer process. Due to this fact the study of combined heat and mass transfer is helpful in understanding of a many technical transfer processes. Arifuzzaman *et al.* [6] studied hydrodynamic stability and heat and mass transfer flow analysis of MHD radiative fourth-grade fluid through porous plate with chemical reaction. Duwairi and Al-Kablawi [7] formulated and analyzed the MHD conjugative heat transfer problem from vertical surfaces embedded in saturated porous media. Seddeek [8] analyzed the effect of variable viscosity and magnetic field on the flow and heat transfer past a continuously moving porous plate. Khalek [9] investigated the effects of mass transfer on steady two-dimensional laminar MHD mixed convection

flow. The heat source/sink effects in thermal convection are significant where there may exist high temperature differences between the surface (e.g. space craft body) and the ambient fluid. Heat generation is also important in the context of exothermic or endothermic chemical reaction. Tania *et al*. [10] has investigated the effects of radiation, heat generation and viscous dissipation on MHD free convection flow along a stretching sheet. Furthermore, Moalem [11] studied the effect of temperature dependent heat sources taking place in electrically heating on the heat transfer within a porous medium. Vajravelu and Nayfeh [12] reported on the hydro magnetic convection at a cone and a wedge in the presence of temperature dependent heat generation or absorption effects. Moreover, Chamkha [13] studied the effect of heat generation or absorption on hydro magnetic three-dimensional free convection flow over a vertical stretching surface. The heat transfer caused by the concentration gradient is called the Dufour effect. The Dufour effects were studied by many researchers. Kafoussias and Williams [14] studied the thermo-diffusion and diffusion-thermo effects on the mixed free-forced convective and mass transfer of steady laminar boundary layer flow over a vertical flat. Afify [15] carried out a numerical analysis to study the free convective heat and mass transfer of an incompressible electrically conducting fluid over a stretching sheet in the presence of suction and injection with the Soret and Dufour effects. Islam and Ahmed [16] investigated effect of thermal diffusion and chemical reaction on MHD free convective flow past an infinite isothermal vertical plate with heat source. Postelnicu [17] analyzed the simultaneous heat and mass transfer by natural convection from a vertical flat plate embedded in an electrically-conducting fluid saturated porous medium using the Darcy Boussinesq model in the presence of Dufour and Soret effects. Nayak *et al.* [18] analyzed Soret and Dufour effects on mixed convection unsteady MHD boundary layer flow over stretching sheet in porous medium with chemically reactive species.

The objective of the present work is to analysis the effect of heat generation parameter and Dufour number on the magneto hydrodynamic (MHD) free convection flow of an electrically conducting incompressible viscous fluid over an inclined plate embedded in a porous medium. The present work is a generalization of the work done by Mangathai *et al.* [19] to consider the Dufour effects and heat source on the flow characteristics.

2.   Formulation of the Problem

Let us consider the unsteady flow of an incompressible viscous fluid past an infinite inclined plate with variable heat and mass transfer. The x'-axis is taken along the plate with the angle of inclination α to the vertical and the y'-axis is taken normal to the plate. The viscous fluid is taken to be electrically conducting and fills the porous half space y' >0. A uniform magnetic field of strength B_0 is applied in the y'-direction transversely to the plate. The applied magnetic field is assumed to be strong enough so that the induced magnetic field due to the fluid motion is weak and can be neglected. According to Cramer and Pai, this assumption is physically justified for partially ionized fluids and metallic liquids because of their small magnetic Reynolds number. Since there is no applied or

polarization voltage imposed on the flow field, the electric field due to polarization of charges is zero. Initially, both the fluid and the plate are at rest with constant temperature T_∞ and constant concentration C_∞. At time $t' > 0$, the plate is given a sudden jerk, and the motion is induced in the direction of flow against the gravity with uniform velocity u_0. The temperature and concentration of the plate are raised linearly with respect to time. Also, it is considered that the viscous dissipation is negligible and the fluid is thick gray absorbing-emitting radiation but non scattering medium. Since the plate is infinite in the (x', z') plane, all physical variables are functions of y' and t' only. The physical model and coordinates system is shown in below
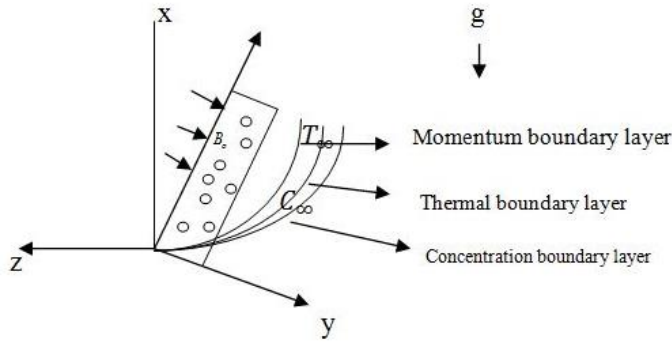
Fig. 1. Geometry of the physical model and co-ordinate system of the problem.

In view of the above assumptions, as well as of the usual Boussinesq's approximation, the governing equations reduce to

$$\frac{\partial u'}{\partial t'} = v \frac{\partial^2 u'}{\partial y'^2} + g\beta(T - T_\infty) \cos\alpha + g\beta_c(C - C_\infty)\cos\alpha - \frac{\sigma B_0^2}{\rho}u' - \frac{v}{K^*}u' \tag{1}$$

$$\frac{\partial T}{\partial t'} = \frac{\kappa}{\rho c_p}\frac{\partial^2 T}{\partial y'^2} - \frac{1}{\rho c_p}\frac{\partial q'}{\partial y'} + \rho\frac{D_M K_T}{C_s}\frac{\partial^2 C}{\partial y'^2} \tag{2}$$

$$\frac{\partial C}{\partial t'} = D_M \frac{\partial^2 C}{\partial y'^2} - K_1(C - C_\infty) \tag{3}$$

The boundary conditions are

$$t' \leq 0 : u' = 0, T = T_\infty, C = C_\infty \text{ for all } y' > 0$$

$$t' > 0 : \quad u' = U_0, T = T_\infty + (T_w - T_\infty)At', \quad C = C_\infty + (C_w - C_\infty)At' \text{ at } y' = 0$$

$$u' = 0, T = T_\infty, C = C_\infty \text{ as } y' \to \infty \tag{4}$$

We adopt the Rosseland approximation for radiative heat flux q_r, namely

$$q' = -\frac{4\sigma^*}{3a^*}\frac{\partial T^4}{\partial y'} \tag{5}$$

Now expanding T^4 in Taylor series about T_∞ and neglecting higher order terms

$$T^4 \cong 4TT_\infty^3 - 3T_\infty^4 \tag{6}$$

To normalize the equations (1)-(3) the following non-dimensional quantities are introduced.

$$u = \frac{u'}{U_0}, t = \frac{t'U_0^2}{v}, y = \frac{y'U_0}{v}, \theta = \frac{T - T_\infty}{T_w - T_\infty}, \varphi = \frac{C - C_\infty}{C_w - C_\infty} \tag{7}$$

The non-dimensional form of the equations (1), (2) and (3) are as follows

$$\frac{\partial u}{\partial t} = \frac{\partial^2 u}{\partial y^2} + Gr\theta \cos \alpha + Gm\varphi \cos \alpha - (M + \frac{1}{K})u \tag{8}$$

$$\frac{\partial \theta}{\partial t} = \frac{1+N}{Pr}\frac{\partial^2 \theta}{\partial y^2} - \frac{N\theta}{Pr} - \frac{Q}{Pr}\theta + D_u \frac{\partial^2 \varphi}{\partial y^2} \tag{9}$$

$$\frac{\partial \varphi}{\partial t} = \frac{1}{Sc}\frac{\partial^2 \varphi}{\partial y^2} - K\varphi \tag{10}$$

The corresponding non dimensional boundary conditions are

$$t \le 0: u = 0, \theta = 0, \varphi = 0 \; for \; all \; y > 0$$
$$t > 0 : \quad u = 1, \theta = t, \varphi = t \quad at \; y = 0$$
$$u \to 0, \theta \to t, \varphi \to t \; \; as \; y \to \infty \tag{11}$$

In order to normalize the mathematical model, we introduce the following non-dimensional quantifies

$$Gr = \frac{vg\beta(T_w - T_\infty)}{U_0^3} \; , Gm = \frac{vg\beta^*(C_w - C_\infty)}{U_0^3} \; , Pr = \frac{\mu c_p}{\kappa} \; , K^* = \frac{a^* U_0^2}{v^2} \; , Sc = \frac{v}{D_M} \; ,$$

$$M = \frac{\sigma B_0^2 v}{\rho U_0^2} \; , K = \frac{K_1 v}{U_0^2} \; , N = \frac{16\sigma T_\infty^3}{3\kappa a^*} \; , Q = \frac{\gamma^2 Q\prime}{KU_0^2} \; , D_u = \frac{D_T K_T (C_w - C_\infty)}{\gamma C_p C_S (T_w - T_\infty)} \tag{12}$$

3. Method of Solution

Consider the velocity field u, temperature distribution θ, concentration profile φ as follows:

$$u = u_0 e^{-\omega t}$$
$$\theta = \theta_0 e^{-\omega t}$$
$$\varphi = \varphi_0 e^{-\omega t}$$

On substitution of (12), in equations (8), (9), and (10)

$$u_0'' - a_3^2 u_0 = -(Gr\theta_0 + Gm\varphi_0)\cos \alpha \tag{13}$$
$$\theta_0'' - a_2^2 \theta_0 = D_u \varphi_0'' \tag{14}$$
$$\varphi_0'' - a_1^2 \varphi_0 = 0 \tag{15}$$

The corresponding boundary conditions become:

$$u_0 = e^{-\omega t} \; , \; \theta_0 = te^{-\omega t} \; , \; \varphi_0 = `te^{-\omega t} \quad at \; y = 0$$
$$u_0 \to 0 \; , \; \theta_0 \to 0 \; , \; \varphi_0 \to 0 \quad as \; y \to \infty \tag{16}$$

The analytical solutions of the equations (13 to 15) subject to the boundary condition (16) are

$$\varphi_0 = te^{-\omega t}e^{-a_1 t} \tag{17}$$

$$\theta_0 = te^{-\omega t}e^{-a_2 t} - \frac{a_3}{(a_1^2 - a_2^2)}e^{-(a_1 + a_2)y} + \frac{a_3}{(a_1^2 - a_2^2)}e^{-a_1 y} \tag{18}$$

$$u_0 = e^{-\omega t}e^{-a_4 t} - a_{10}e^{-(a_4 + a_2)y} - a_{11}e^{-(a_4 + a_2 + a_1)y} - a_{12}e^{-(a_4 + a_1)y} + a_{10}e^{-a_2 y} + a_{11}e^{-(a_1 + a_2)y} + a_{12}e^{-a_1 y} \tag{19}$$

In view of the above solutions, the velocity, temperature and concentration distribution in the boundary layer become as

$$u = e^{-a_4 t} - a_{10}e^{-(a_4 + a_2)y + \omega t} - a_{11}e^{-(a_4 + a_2 + a_1)y + \omega t} - a_{12}e^{-(a_4 + a_1)y + \omega t}$$

$$+ a_{10}e^{-a_2 y + \omega t} + a_{11}e^{-(a_1 + a_2)y + \omega t} + a_{12}e^{-a_1 y + \omega t}$$

$$\theta = te^{-a_2 t} - \frac{a_3}{\left(a_1^2 - a_2^2\right)} e^{-(a_1 + a_2)y + \omega t} + \frac{a_3}{\left(a_1^2 - a_2^2\right)} e^{-a_1 y + \omega t}$$

$$\varphi = te^{-a_1 t} e^{\omega t}$$

4. Skin Friction

The non-dimensional form of skin friction coefficient at plate is given by

$$\tau = e^{-a_4 t} + a_{10}\left(a_4 + a_2\right)e^{\omega t} + a_{11}\left(a_4 + a_2 + a_1\right)e^{\omega t} + a_{12}\left(a_4 + a_1\right)e^{\omega t}$$
$$- a_{10}a_2 e^{\omega t} - a_{11}\left(a_1 + a_2\right)e^{\omega t} - a_1 a_{12} e^{\omega t}$$

5. Nusselt Number

The coefficient of the rate of heat transfer in terms of Nusselt number is given by

$$Nu = -a_2 t + \frac{a_3\left(a_1 + a_2\right)}{\left(a_1^2 - a_1^2\right)} e^{\omega t} + \frac{a_3 a_1}{\left(a_1^2 - a_1^2\right)} e^{\omega t}$$

6. Sherwood Number

The expressions for mass transfer at the plate in terms of Sherwood number is given by
$$Sh = -a_1 t$$

7. Results and Discussion

In order to get the physical insight into the problem, we have studied the influence of various parameters like Hartmann number (M), heat source parameter (Q), radiation parameter (N), Dufour number (Du), Schmidt number (Sc), thermal Grashof number (Gr), Prandtl number (Pr), permeability parameter (K) on velocity field, temperature profile, concentration distribution and skin friction at the plate in Figs. (2-10) while keeping the other parameters fixed.

Fig. 2a shows the effect of magnetic field strength on the momentum boundary layer thickness is illustrated. It is now a well-established fact that the magnetic field presents a damping effect on the velocity field by creating drag force that opposes the fluid motion, causing the velocity to decrease. Fig. 2b indicates the variation of the velocity boundary-layer with the heat generation/absorption parameter (Q). It is noticed that the velocity boundary layer thickness decreases with an increase in the generation/absorption parameter.

The influence of radiation parameter (N) on the velocity field is shown by Fig. 3a. It is seen that the fluid velocity decelerate with an increase in the radiation parameter. Fig. 3b shows the variation of the velocity boundary-layer with the Dufour number (Du). It is observed that the velocity boundary layer thickness increases with an increase in the Dufour number.
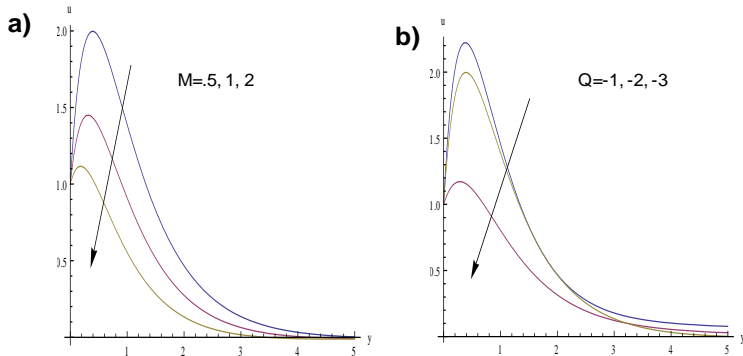
Fig. 2. Velocity profiles for different values of a) M and b) Q. Gr = 5, Gm = 2, K= 0.5, ω = 0.1, t=1, N= 0.5, Q = -1, Pr = 0.71, Sc = 0.60, γ=1, Du=1, $\alpha = \frac{\pi}{3}$
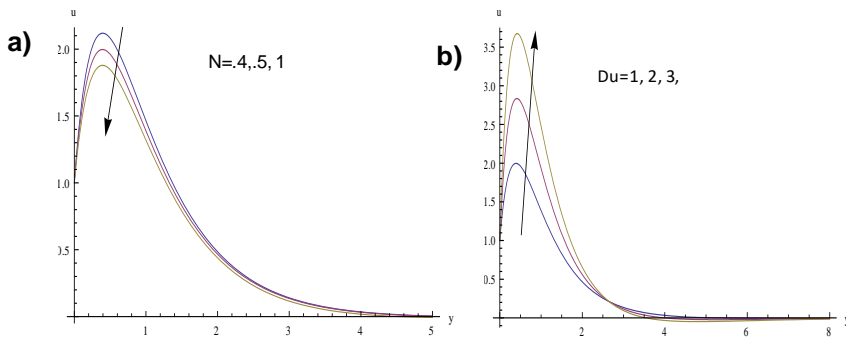

Fig. 3. Velocity profile for different values of a) N: Gr = 5, Gm = 2, K = 0.5, ω=0.1, t=1, $\alpha = \frac{\pi}{3}$, Q= -1, Pr = 0.71, Sc = 0.60, γ = 1, Du = 1; and b) Du: Gr = 5,Gm = 2, K = 0.5, ω = 0.1, t = 1, N = 0.5, Q = -1, Pr = 0.71, Sc = 0.60, γ=1, $\alpha = \frac{\pi}{3}$.
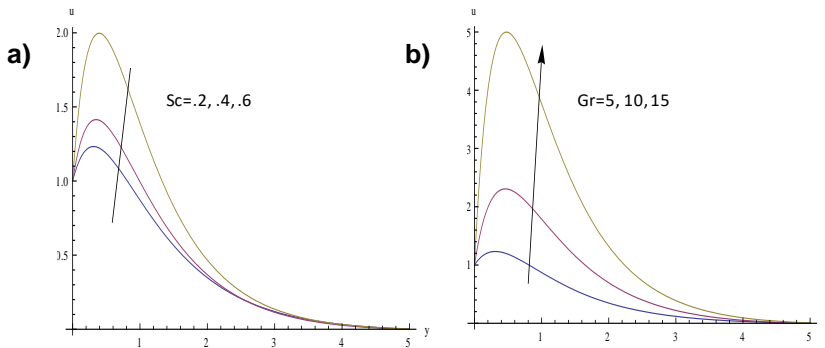

Fig. 4. Velocity profile for different values of a) Sc: Gr = 5, Gm = 2, K = 0.5, ω = 0.1, t = 1, N = 0.5, Q = -1, Pr = 0.71, γ = 1, Du = 1, $\alpha = \frac{\pi}{3}$; and b) Gr: Gm = 2, K = 0.5, ω = 0.1, t = 1, N = 0.5, $\alpha = \frac{\pi}{3}$, Q = -1, Pr = 0.71, Sc = 0.60, γ = 1, Du = 1.

Fig. 4a illustrates the effect of the Schmidt number (*Sc*) on the velocity. It is noticed that as Schmidt number (*Sc*) increases the velocity field increases. Fig. 4b illustrates the effect of the thermal Grashof number (*Gr*) on the velocity field. The thermal *Gr* signifies the relative effect of the thermal buoyancy force to the viscous hydrodynamic force. The flow is accelerated due to the enhancement in buoyancy force corresponding to an increase in the thermal *Gr*.
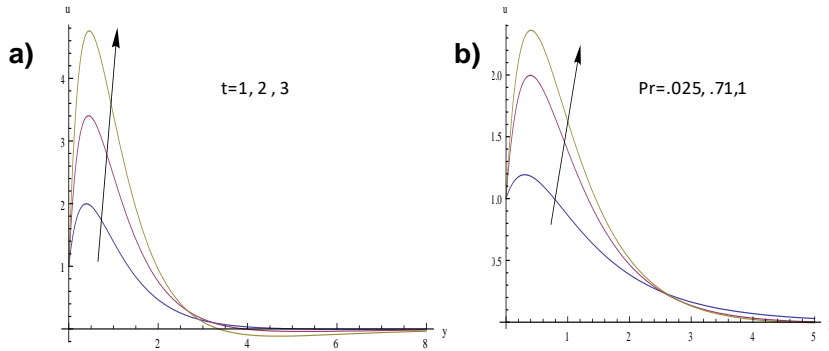

Fig. 5. Velocity profiles for different values of a) t: Gr = 5, Gm = 2, K = 0.5, ω = 0.1, N = 0.5, $\alpha = \frac{\pi}{3}$, Q = -1, Pr = 0.71, Sc = 0.60, γ = 1, Du = 1; and b) Pr: Gr = 5, Gm = 2, K = 0.5, ω = 0.1, t = 1, N = 0.5, Q = -1, Sc = 0.60, γ = 1, Du = 1, $\alpha = \frac{\pi}{3}$.

Fig. 5a shows the influence of dimensionless time *t* on the velocity profiles. It is found that velocity is an increasing function of time. Fig 5b shows the trend of slight increase in the fluid velocity near the vertical plate is observed with an increase in Prandtl number (*Pr*).
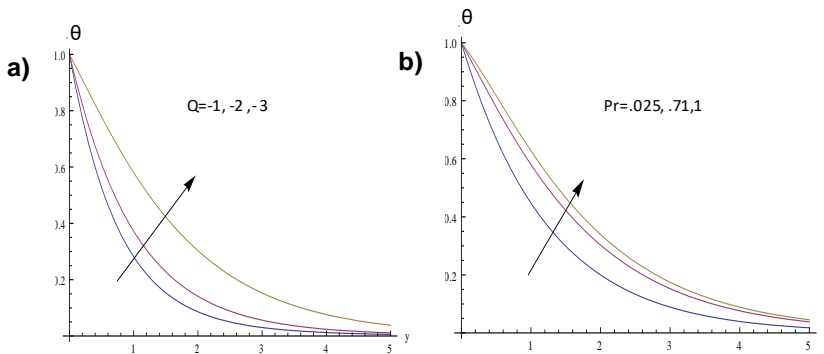

Fig. 6. Temperature profiles for different values of a) Q: Gr = 5, Gm = 2, K = 0.5, ω = 0.1, t = 1, N = 0.5, Pr = 0.71, Sc = 0.60, γ = 1, Du=1, $\alpha = \frac{\pi}{3}$; and b) Pr: Gr = 5, Gm = 2, K = 0.5, ω = 0.1, t = 1, N = 0.5, Q= 1, Sc = 0.60, γ = 1, Du = 1, $\alpha = \frac{\pi}{3}$.

Fig. 6a illustrates the effect of the heat generation/absorption parameter (Q) on the temperature. It is noticed that as the heat generation/absorption parameter increases, the temperature increases. Fig. 6b illustrates the effect of the Prandtl number (Pr) on the temperature. It is noticed that as the Pr increases, the temperature increases.
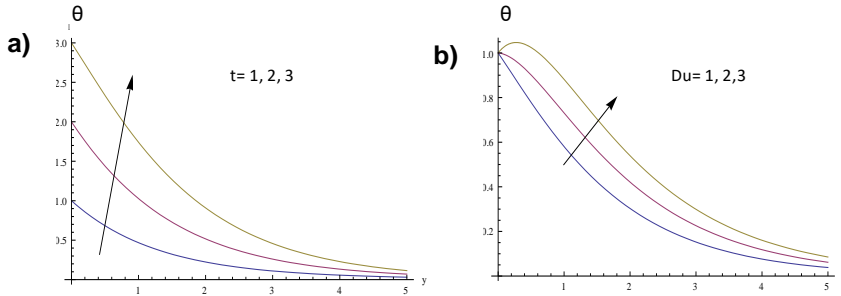

Fig. 7. Temperature profile for different values of a) t: Gr = 5, Gm = 2, K = 0.5, ω = 0.1, N = 0.5, $\alpha = \frac{\pi}{3}$, Q = -1, Pr = 0.71, Sc = 0.60, γ = 1, Du = 1; and b) Du: Gr = 5, Gm = 2, K = 0.5, ω = 0.1, t = 1, N = 0.5, Q= -1, Pr = 0.71, Sc = 0.60, γ=1, $\alpha = \frac{\pi}{3}$.

Fig. 7a is plotted to show the effects of the dimensionless time t on the temperature. Obviously, the temperature increases with increasing time. This graphical behavior of temperature can be also verified from the boundary condition of the temperature field shown in Eq. 12. Hence, the accuracy is checked and again, we are confident that the analytical result for temperature is correct. Fig. 7b shows the variation of the temperature profile with the Dufour number (Du). It is noticed that the thermal boundary layer thickness increases with an increase in the Du.
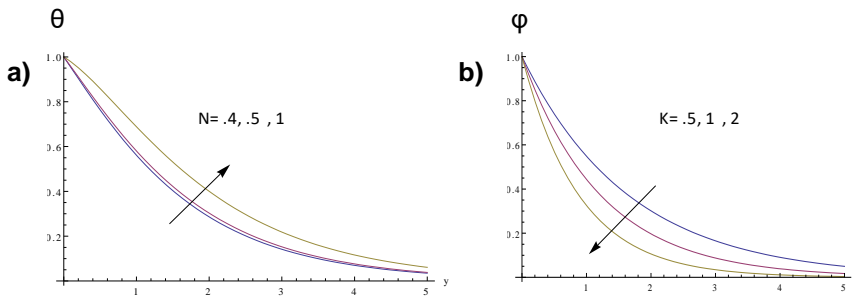

Fig. 8. Temperature profiles for different values of a) N: Gr = 5, Gm = 2, K = 0.5, ω = 0.1, t = 1, $\alpha = \frac{\pi}{3}$, Q = -1, Pr = 0.71, Sc = 0.60, γ = 1, Du=1; and b) K: Gr = 5, Gm = 2, ω = 0.1, t = 1, N = 0.5, $\alpha = \frac{\pi}{3}$, Q = -1, Pr = 0.71, Sc = 0.60, γ = 1, Du = 1.

Furthermore, the temperature profiles for increasing values of radiation parameter (N) indicate an increasing behavior as shown in Fig. 8a. A similar behavior is also expected because the radiation parameter (N) signifies the relative contribution of conduction heat

transfer to thermal radiation transfer, Fig. 8b shows the physical effect of chemical reaction parameter (K) which clearly demonstrates that concentration profiles decrease rapidly when K is increased.
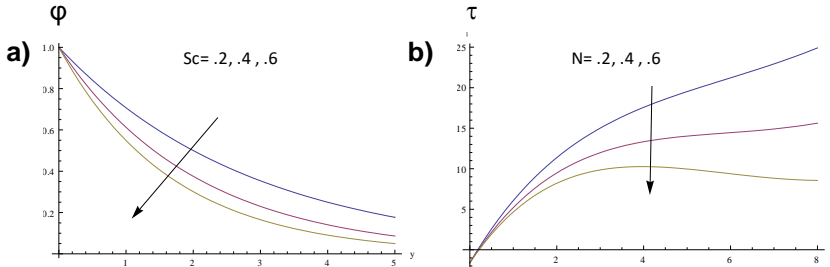

Fig. 9. a) Concentration profile for different values of Sc: Gr = 5, Gm = 2, K = 0.5, ω = 0.1, t = 1, N = 0.5, Q = -1, Pr = 0.71, γ=1, Du=1, $\alpha = \frac{\pi}{3}$; and b) skin friction for different values of N: Gr = 5, Gm = 2 ,K = 0.5, ω = 0.1, t = 1, $\alpha = \frac{\pi}{3}$, Q = -1, Pr = 0.71, Sc = 0.60, γ = 1, Du = 1.

Fig. 9a illustrates the effect of Schmidt number (*Sc*) on the concentration. It is noticed that as the *Sc* increases, there is a decreasing trend in the concentration field.
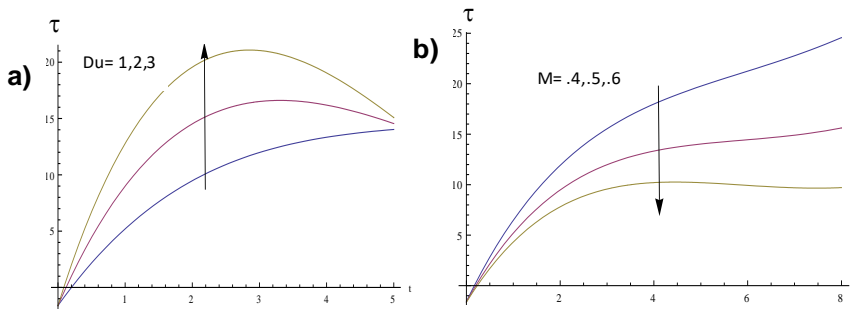

Fig. 10. Skin frictions for different values of Du: Gr = 5, Gm = 2, K = 0.5, ω = 0.1, t = 1, N = 0.5, Q = -1, Pr = 0.71, Sc = 0.60, γ = 1, Du = 1, $\alpha = \frac{\pi}{3}$; and b) M: Gr = 5, Gm = 2, K = 0.5, ω = 0.1, t = 1, N = 0.5, Q = -1, Pr = 0.71, Sc = 0.60, γ = 1, Du = 1 , $\alpha = \frac{\pi}{3}$.

Variations of skin friction against *t* for different values of radiation, diffusion thermo effect, Hartmann number are shown in the Figs. 9b, 10a and 10b. It is noticed that the local skin-friction coefficient increases with an increase in *Du* but decreases with an increase in radiation parameter and Hartmann number.

8. Code Validation

For the accuracy of the results, the present study is compared with the previous study of Mangathai *et al.* [18] as shown in Fig. 11. It is observed that, in the absence of Dufour effect and heat source, the result obtained in our present work are in good agreement with that of Mangathai *et al.* [18]. Fig. 12 shows the effect of magnetic field parameter *M*

(when $Du = 0$ and $Q = 0$) on the velocity profile and the result is compared with Fig. 11 (Fig. 2a of the work Mangathai *et al.* [18]). It is observed that both the figures exactly coincide, depicting similar result that the velocity decreases with the application of transverse magnetic field.
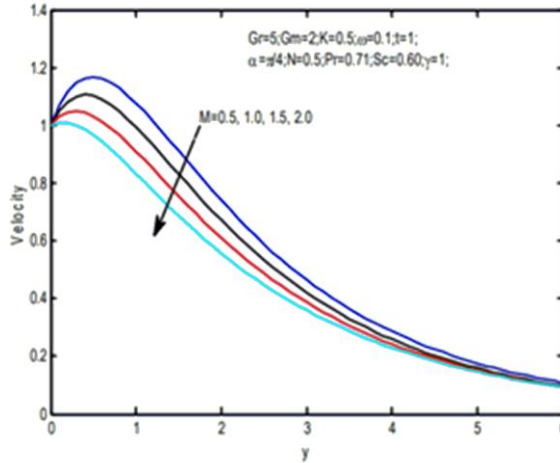

Fig. 11. Velocity versus y for Gr = 5, Gm = 2, K = 0.5, ω = 0.1, t = 1, N = 0.5, Q=0, $\boldsymbol{\alpha} = \frac{\pi}{4}$, Pr = 0.71, Sc = 0.60, γ = 1, Du=0.
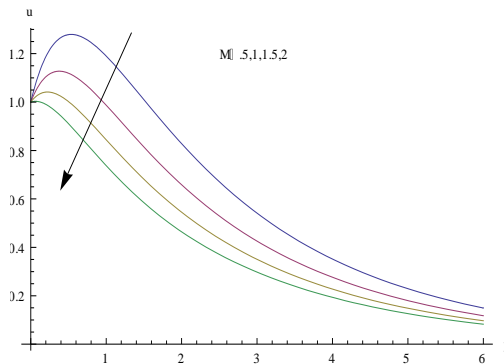
Fig. 12. Velocity versus y for Gr = 5, Gm = 2, K = 0.5, ω = 0.1, t = 1, N = 0.5, Q = 0, $\boldsymbol{\alpha} = \frac{\pi}{4}$, Pr = 0.71, Sc = 0.60, γ = 1, Du = 0.

5. Conclusion

In this problem, we investigate the effects of Schmidt number, heat source parameter, thermal Grashof number, radiation parameter, Hartmann number, Dufour number and Prandtl number and chemical reaction on a steady MHD mixed convective fluid flow past a continuously moving infinite vertical porous plate under the influence of a transversely

applied magnetic field in presents of heat source. The non-dimensional governing equations are solved with the help of perturbation technique and results are reported in terms of graphs.

The velocity profile decreases with the increase of Hartmann number, heat source parameter, radiation parameter whereas the velocity profile increases with the increasing values of Dufour number, Schmidt number, Grashof number, dimensionless time, Prandtl number.The fluid temperature increases with the increase of heat source parameter, Prandtl number, dimensionless time, Dufour number and radiation parameter.The concentration profile decreases with the increase of Chemical reaction, Schmidt number. The coefficient of skin friction decreases due to the increase of thermal radiation and Hartmann number in contrast the viscous drag at the plate enhance with the increasing values of Dufour number.

References

1. A. Raptis, C. Perdikis, H. S. Takhar, Appl. Math. Comput. **153**, 645 (2004). https://doi.org/10.1016/S0096-3003(03)00657-X
2. J. T. Yen and C. C. Chang, The Physics Fluids **4** (1961).
3. A. J. Chamkha, Int. J. Eng. Sci. **42**, 217 (2004). https://doi.org/10.1016/S0020-7225(03)00285-4
4. T. R. Mahapatra, S. K. Nandy, and A. S. Gupta, Int. J. Non-Linear Mechanics **215**, 1696 (2009). https://doi.org/10.1016/j.amc.2009.07.022
5. M. J. H. Munshi and M. A. Alim, J. Sci. Res. **9**, 1 (2017). https://doi.org/10.3329/jsr.v1i1.27702
6. S. M. Arifuzzaman, M. S. Khan, A. Al-Mamun, S. Reza-E-Rabbi, P. Biswas, and I. Karim, J. King Saud Univ. – Sci. **31**, 1388, (2019). https://doi.org/10.1016/j.jksus.2018.12.009
7. Y. M. Al-Badawi and H. M. Duwairi, Appl. Math. Mech.-Engl. Ed. **31**, 1105 (2010). https://doi.org/10.1007/s10483-010-1346-6
8. M. A. Seddeek, Int. Commun. Heat Mass **27**, 1037 (2000). https://doi.org/10.1016/S0735-1933(00)00183-4
9. M. M. Abdelkhalek, Int. Commun. Heat Mass **33**, 249 (2006). https://doi.org/10.1016/j.icheatmasstransfer.2005.09.008
10. T. S. Khaleque and M. A. Samad, Res. J Appl. Sci., Eng. Technol. **2**, 368 (2010).
11. D. Moalem, Int. J. Heat Mass Transfer **19**, 529 (1976). https://doi.org/10.1016/0017-9310(76)90166-6
12. K. Vajrevelu and J. Nayfeh, Int. Comm. Heat Mass Transfer **19**, 701 (1992). https://doi.org/10.1016/0735-1933(92)90052-J
13. A. J. Chamkha, Int. J. Heat Fluid Flow **20**, 84 (1999). https://doi.org/10.1016/S0142-727X(98)10032-2
14. N. G. Kafoussias and E. W. Williams, Int. J. Eng. Sci. **33**, 1369 (1995). https://doi.org/10.1016/0020-7225(94)00132-4
15. A. A. Afify, Commun. Nonlinear Sci. Numer. Simul. **14**, 2202 (2009). https://doi.org/10.1016/j.cnsns.2008.07.001
16. S. H. Islam and N. Ahmed, Ital. J. Pure Appl. Math. **42**, 559 (2019).
17. A. Postelnicu, Int. J. Heat Mass Transfer **47**, 1467 (2004). https://doi.org/10.1016/j.ijheatmasstransfer.2003.09.017
18. A. Nayak, S. Panda, and D. K. Phukan, Appl. Math. Mechanics **35**, 849 (2014). https://doi.org/10.1007/s10483-014-1830-9
19. P. Mangathai, G. V. R. Reddy, and B. R. Reddy, Int. J. Adv. Comput. Math. Sci. **7**, 1 (2015).

Appendix

$$a_1{}^2 = Sc(K + \omega), \quad a_2{}^2 = \frac{\omega Pr}{(1 + N)} - \frac{Q}{(1 + N)}$$

$$a_3 = \frac{- Pr \, D_u a_1{}^2 t}{(1 + N)e^{\omega t}}, \qquad a_4{}^2 = \left(M + \frac{1}{K_p} + \omega \right)$$

$$a_5 = -Gr \cos \alpha \, t e^{-\omega t}, \qquad a_6 = -Gr \cos \alpha \frac{a_3}{a_1{}^2 - a_2{}^2}$$

$$a_7 = Gr \cos \alpha \frac{a_3}{a_1{}^2 - a_2{}^2}, \qquad a_8 = -Gm \cos \alpha \, t e^{-\omega t}$$

$$a_9 = a_6 + a_8, \qquad a_{10} = \frac{a_5}{a_2{}^2 - a_4{}^2}$$

$$a_{11} = \frac{a_7}{(a_{1+}a_2)^2 - a_4{}^2}, \qquad a_{12} = \frac{a_9}{a_1{}^2 - a_4{}^2}$$